Desalination 573 (2024) 117180

Contents lists available at ScienceDirect

Desalination

journal homepage: www.elsevier.com/locate/desal

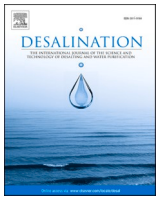

ANN based-model for estimating the boron permeability coefficient as boric acid in SWRO desalination plants using ensemble-based machine learning

Nabil I. Ajali-Hernández [a,*], A. Ruiz-García [b], Carlos M. Travieso-González [a,c]

[a] Institute for Technological Development and Innovation in Communications (IDeTIC), University of Las Palmas de Gran Canaria, Campus Universitario de Tafira, Las Palmas de Gran Canaria 35017, Spain
[b] Department of Electronic Engineering and Automation, University of Las Palmas de Gran Canaria, Campus Universitario de Tafira, Las Palmas de Gran Canaria 35017, Spain
[c] Signals and Communications Department (DSC), University of Las Palmas de Gran Canaria, Campus Universitario de Tafira, Las Palmas de Gran Canaria 35017, Spain

HIGHLIGHTS

- Predicting the Boron Permeability Coefficient of Seawater in a Reverse Osmosis Desalination Plant Using Machine Learning
- Analysis of different input conditions for prediction in SWRO systems with multiple membrane elements varying conditions
- Ensemble-based machine learning model for prediction of boron rejection permeability coefficient
- Calculation of boron rejection concentration from boron permeability coefficient

ARTICLE INFO

Keywords:
Desalination
Reverse osmosis
Boron rejection
Neural networks
Machine learning

ABSTRACT

This study examines the relationship between input conditions and the prediction of boron rejection in full-scale seawater reverse osmosis (SWRO) desalination plants using ensemble-based machine learning. While reverse osmosis is the dominant desalination technology, limited research has focused on analyzing plant performance under actual operating conditions. To address this gap, we developed and implemented machine learning algorithms to forecast boron permeability coefficient values, which are indicative of boron rejection concentrations in the permeate. Our analysis utilizes data from a SWRO desalination plant in southeast Spain, examining various input variables and their influence on the prediction of these parameters. The results demonstrate that our ensemble-based machine learning approach can predict boron permeability coefficient values with a reasonable margin of error of 1 mgL^{-1}, as evidenced by mean average error (MAE) and mean absolute percentage error (*MAPE*) values of 7.93·10–8 and 11.8 %, respectively. In conclusion, an innovative application of artificial intelligence algorithms in the field of water purification under real operational conditions has been introduced, thus introducing valuable insights into the use of machine learning algorithms for forecasting boron rejection concentrations in full-scale SWRO desalination plants. The findings lay the foundation for future researches exploring automated and deep-learning methods in water purification.

1. Introduction

Water scarcity is one of the main challenges for human life and has stimulated the use of desalination technologies to produce water for different purposes. Among the available technologies, reverse osmosis (RO) is in the lead due to its reliability [1,2] and lower specific energy consumption in comparison with other technologies [3,4]. Unfortunately, RO has some weak points such as loss of performance due to the fouling of RO membranes [5–7] and low rejection rates of some ions that can be toxic to humans such as boron, fluorine, etc. [8,9]. This has led to significant efforts being made to improve the selectivity of RO membranes, trying not to penalize the production of permeate per unit of membrane-active surface [10,11]. Usually, the determination of ion concentration in the permeate (C_{pB}) is carried out in a laboratory so it is not measured in real-time. This can be problematic because it is not known in real time how a change in operating conditions affects the ion permeability coefficients (B_j) and consequently the C_{pB}. It is important to

* Corresponding author.
E-mail address: nabil.ajali101@alu.ulpgc.es (N.I. Ajali-Hernández).

https://doi.org/10.1016/j.desal.2023.117180
Received 5 September 2023; Received in revised form 7 November 2023; Accepted 19 November 2023
Available online 28 November 2023

Nomenclature

Acronyms

ANN	Artificial neural network
HL	Hidden layer
RO	Reverse osmosis
PV	Pressure vessel
PF	Polarization factor
SWRO	Seawater reverse osmosis
$Cond_f$	Feed conductivity (μS cm^{-1})
$Cond_p$	Permeate conductivity (μS cm^{-1})
B_B	Boron ion permeability coefficient (m d^{-1})
C	Concentration (mg L^{-1})
D	Solute diffusivity (m^2 s^{-1})
EPS	Average element permeate flow (m^3 d^{-1})
J	Flow per unit area (m^3 m^{-2} d^{-1})
k	Mass transfer coefficient
m	Molal concentration (mol kg^{-1})
P	Permeability coefficient (m d^{-1})
p	Pressure (Pa)
Q	Flow (m^3 d^{-1})
R	Flow recovery (%)
S_m	Membrane surface(m^2)
T	Temperature (°C)
T_B	Rejection temperature
TCF	Temperature correction factor
TDS	Total dissolved solids (mg L^{-1})
tf	Operating time factor

Greek letters

Δp	Pressure gradient (Pa)
η	Dynamic viscosity (kg m^{-1} s)
ν	Velocity (m s^{-1})
π	Osmotic pressure (Pa)
ρ	Density (kg m^{-3})
σ	Standard deviation

Superscript

0	Membrane manufacturer testing conditions

Subscripts

0	Initial conditions
b	Brine
fb	Feed-brine
f	Feed
m	Membrane
p	Permeate
S	Solute
w	Water

develop predictive models that estimate the C_{pB} in real time [12,13]. In this way, the desalination plant could be working in a proper range operation to meet the permeate quality criteria. It is known that even considering constant the coefficient B, ion rejection depends on the operating parameters [14]. To evaluate ion rejection, it is necessary to determine the variation of B_j with the operating conditions. Modeling B_j is a complex task, as it requires a full understanding of the membrane process [15]. This is difficult from a mathematical perspective as detailed knowledge about membrane and solution properties is needed. In addition to this, it is necessary to obtain a large amount of information in real-time from the RO system which helps to estimate the values of B_j. Machine learning techniques such as artificial neural network (ANN) based models do not require much understanding of the system and allow the modeling of complex and nonlinear systems [16,17].

1.1. Related works

The ANN-based models have been used to predict solute rejection in nanofiltration (NF) and RO process, which processes are roughly similar in terms of transport phenomena. Bowen et al. [18] used ANNs based model to predict the rejection of single salts (NaCl, Na_2SO_2, $MgCl_2$, and $MgSO_4$) and mixtures of these salts by a spiral wound NF membrane in a pilot-scale plant. The input used were; the feed pressure (p_f), pH, ion diffusivity, ion valence, and feed concentration (C_f), and the output was the ion rejection. The network architecture (NA) included 14 inputs, 1 hidden layer (HL) with 12 neurons, and 4 outputs (ions rejection). The activation function was log-sigmoid, the training algorithm the scaled conjugate gradients, and the performance was measured using the mean square error (*MSE*), with an average value of $1.751{\cdot}10^{-5}$. Later, in other work using ANNs, the rejection of two salts (NaCl and $MgCl_2$) at a usual concentration in seawater was evaluated by Darwish et al. [19] using ANNs. Three NF membranes were used (NF90, NF270, and N30F from Filmtec™). p_f, permeate flow (Q_p), and C_f were used as inputs, an HL with 4 neurons and one output, the same activation function as in the previously mentioned study, and Bayesian regularization as the training algorithm. An average absolute percentage deviation of up to 5 % for $MgCl_2$ and up to 3 % for NaCl was obtained.

Al-Zoubi et al. [20] studied the performance of two NF membranes (NF90 and NF270) in terms of solute (KCl, Na_2SO_4, and $MgSO_4$) rejection using ANNs (perceptron). The predictions obtained with ANNs were compared with those estimated using the Spiegler-Kedem model. The calculated NA was formed by 3 inputs, 1 HL with 4 neurons, and 1 output. Q_p, p_f, and C_f were used as inputs, and absolute deviations <8 % were obtained. Another work of Yangali- Quintanilla et al. [21] proposed an ANN based model on a quantitative structure–activity relationship (QSAR) equation that defines an appropriate set of solute and membrane variables capable of representing and describing rejection. NF and RO membranes as flat sheets in a cross-flow cell were used to generate 6 simple ANN-based models (perceptron). Organic salt rejections were evaluated by considering the salt rejection of the membranes, molecular length, equivalent width, and hydrophobicity as inputs, 1 HL with 2–3 neurons, and 1 output. The activation function used was tanh-sigmoid, the training algorithm was Levenberg-Marquardt, and error functions such as mean average absolute error (*AAE*), absolute percent error (*MAPE*), maximum absolute percent error (*MaxAPE*), and standard deviation of the error (*STDE*) were used for training, validation and prediction. Regarding the prediction, the range of obtained values was; $AAE = 4.56–10.33$, $MAPE = 0.14–0.64$, $MaxAPE = 0.83–14.66$, and $= 5.32–13.29$ %.

Other works in laboratory or pilot plant scale conditions, such as those of Khaouane et al. [22], Murthy and Vora [23] or Libotean et al. [24], repeat this type of simple architectures using ANN type networks to obtain results with controlled conditions resulting in values of <2 %.

Khayet et al. [25] developed predicting models (for the estimation of NaCl rejection and Q_p) using response surface methodology (RSM) and ANN. A RO pilot plant was used in this study considering C_f, T_f), p_f, and Q_f as inputs. The activation function used was log-sigmoid, Levenberg-Marquardt as the training algorithm, and the NA was formed by the mentioned inputs, 2 HL with 5 and 3 neurons respectively, and 1 output. *MSE* was used as a performance function, and the coefficient of multiple determination (R^2) concerning the performance prediction was 1. It was concluded that ANN provided a global model describing RO performance for a wide range of C_f being an advantage over the RSM model however, ANN methodology requires a greater number of experiments

in comparison with RSM.

The use of artificial intelligence applied to large-scale RO plants is finally coming in 2015, where Madaeni et al. [26] developed an ANN-based model for estimating Q_p and permeate conductivity ($Cond_p$). Their architecture used 4 inputs (operating time (t), transmembrane pressure (TMP), feedwater conductivity ($Cond_f$) and Q_f), 2 HL with 11 and 5 neurons respectively and 2 outputs formed the NA. The activation function used was log-sigmoid and Levenberg-Marquardt as the training algorithm. In terms of the performance of the model, R^2 values of 0.94 and 0.99 were obtained for the estimation of Q_p and $Cond_p$ respectively. Choi et al. [27] also carried out an analysis and modeling of the long-term performance of a full-scale RO desalination plant. The models evaluated were based on ANN and tree. The NA of the ANN model had 5 inputs, 1 HL with 10 neurons and 1 output for predicting relative p_f; relative pressure drops (Δp), and relative $Cond_p$. Levenberg-Marquardt was the training algorithm and the precision of the proposed model was measured through the $STDE$ and R^2, both parameters were in a range of 0.014 and 0.065, and between 0.92, and 0.95 respectively.

Research lines focused on ANN and backpropagation are on the rise today. Another example is the work proposed by Asma et al. [28], where the performance of seawater hybrid NF/RO desalination plant including permeate conductivity; permeate flow, and permeate recovery is analyzed under different parameters (time, feed temperature, feed pressure, feed conductivity, and feed flow). An ANN based on back-propagation (Levenberg–Marquardt training algorithm) is used. The ANN architecture is 5–8-3 with a hyperbolic tangent transfer function in the HL and a linear transfer function at the output layer. Results show a good agreement between the prediction and the experimental data during the training with reasonable statistical metrics values ($RMSE$, MAE, and $AARD$). The coefficients of determination values for the prediction of $Cond_p$, permeate flow, and recovery by ANN were 0.969, 0.942, and 0.963, respectively. Hence, the performance of the NF/RO hybrid seawater desalination plant was successfully predicted using the ANN model. Mahadeva et al. [29] on the other hand, obtain yields with a regression of $R^2 = 99.4$ % and error = 0.003 using MATLAB/Simulink software and an ANN network with 2 HL and 20 neurons. They use a short training set and divide the data into 80 train, 10 validation, and 10 test. Once again, good yields of the prediction of these plants using ANN are observed. However, all these works, although they predict performance well, are not optimized since they have laboratory conditions or a short training set.

Hence, there are not many studies that consider the long-term operation of large-scale RO desalination plants, which is important to obtain models closer to the real operation. Especially when the ions present may be toxic and are not highly rejected by RO membranes. In addition, other disadvantages of not considering the long-term operation of large scales in desalination plants include the operation time along with the fouling and the operating parameters, since the permeability coefficients could vary [30]. This can lead to uncertainty about the most appropriate operating regime for the plant in terms of permeate quality. Furthermore, the design of the AI models used in these studies is quite simple and not very robust, with a low number of inputs and a low number of hidden neurons. Deep learning methods [31] and multilayered recurrent neural networks [32] have been shown to improve traditional neural networks and could improve the confidence of predictions obtained in realistic contexts.

In general, artificial intelligence is being applied to desalination plants and it is a topic that is being heavily investigated. But not only in plants that use RO there are also studies in desalination using solar energy. E.g., the study proposed by Salem et al. [33], use AI regression models to predict the efficiency of water desalination, which depends on solar thermal energy. They use a wide range of regression algorithms, including multilayer perceptron (MLP), decision trees (DT), and Bayesian Ridge Regression (BRR). Obtaining ranges of Root Mean Square error ($RMSE$) values of 0.07171–8.05636 and Max Error 0.10108–14.19858 when using independent integer variables.

This paper introduces a pioneering contribution to the domain of salinity in water treatment, presenting an original and comprehensive approach. Unlike previous studies, as depicted in Table 1, the dataset utilized encompasses over 40,000 operating hours, reflecting real-scale operational conditions rather than laboratory, pilot plant, or small-scale settings. Thus, this work represents an initial step towards more precise future research directions.

The second novelty lies in the utilization of advanced methodologies that surpass conventional techniques such as simple multilayer perceptron or simple ANNs architectures, support vector machines, or decision trees. Instead, a more intricate and robust architecture is employed in this study.

Moreover, it should be emphasized that the estimated parameters differ from those measured in previous studies, rendering direct comparisons difficult. As a pioneering investigation, the primary objective is to establish an approach capable of accurately determining the boron permeability coefficient (B_B) and providing estimations within an acceptable margin of error (1 mg L^{-1}), which corresponds to a value lower than 20 %. Finally, the significance of this study is underscored by the fact that the measurements are conducted in real-time, enabling the assessment of only the target parameter without real-time data on other potentially influential substances. This aspect is attributed to the use of experimental data of a full-scale SWRO desalination plant.

Therefore, this paper presents a groundbreaking contribution to the water purification field by introducing and analyzing a dynamic model based on ANNs. This model estimates B_B as boric acid in large-scale SWRO desalination plants, an aspect that has not been previously explored. The study utilizes long-term operational data from a large-scale SWRO desalination plant, covering over 1500 operating days

Table 1
Summary of related works and their conditions.

	Conditions	Architecture (layers)	Estimated parameter	Metrics
Bowen et al. [18]	Pilot plant scale	Simple ANN (14-1-12)	NaCl, Na_2SO_2, $MgCl_2$, and $MgSO_4$	$MSE = 1751{\cdot}10^{-5}$
Darwish et al. [19]	Seawater concentration	Simple ANN (4-1-4)	$MgCL_2$ and NaCl	MAE = 5–3 %
Al-Zoubi et al. [20]	Laboratory	Simple ANN (3-1-1) perceptron	KCl, Na_2SO_4, and $MgSO_4$	Error < 8 %
Yan. et al. [21]	Laboratory	Simple ANN models	>50	MAE = 4,56–10,33 and $MAPE$ = 0,14-0,64
Khaouane et al. [22]	Laboratory	Bidirectional ANN	42 organic compounds	$RMSE$ = 5,33
Murthy y Vora [23]	Laboratory	Simple ANN model	NaCl	MAE = 1–1.5 %
Libotean et al. [24]	Pilot plant scale	Simple ANN model (8-1-1)	NaCl	MAE = 0,049 %
Khayet et al. [25]	Pilot plant scale	ANN (4-2-1) multi-layer	NaCl	$R^2 = 1$
Madaeni et al. [26]	Full-scale RO plant, (5000 h)	ANN (4-2-2) multi-layer	Qp and Condp	R^2 = 0,94-0,99
Choi et al. [27]	Full-scale RO desalination plant (16.000 h)	Simple ANN model (5-1-1) and Tree	pf; relative pressure drops (Δp), and relative Cp	R^2 = 0,92-0,95
Asma et al. [28]	Small-scale NF/RO seawater	ANN (5-8-3) multi-layer	Qp, Condp and R	$RMSE$ = 0,969 and MAE = 0,963

and employing Toray Company's TM820L-440 and TM820S-400 membrane modules. By employing machine learning algorithms to predict boron permeability coefficient values in the permeate and obtain boron rejection concentrations, this study introduces a novel approach in the field. The designed stable neural network architecture provides accurate predictions of C_{pB}. These findings underscore the significance of considering operating conditions when analyzing SWRO desalination plants and highlight the potential of machine learning algorithms in enhancing their efficiency. This study represents a significant advancement towards the development of automated and deep learning methods for water purification, which are expected to exert a substantial impact on the water industry in the foreseeable future.

2. Materials and methods

2.1. Plant description and experimental dataset

The plant is located in the southeast of Spain and has been in operation since 2009. The raw water is taken from 18 coastal wells with a depth between 50 m and 100 m. Each well with a submersible pump can pump 360 $m^3\,h^{-1}$ with a pressure of 0.27 MPa. The pre-treatment system of the plant consists of 10 gravity sand filters, antiscalant dosing at a concentration of 0.5 ppm, and 6 cartridge filters with a porosity of 5 μm. Additionally, the plant utilizes 11 high-pressure pumps, with 2 pumps kept in reserve, equipped with Pelton turbines to recover energy. The SWRO system comprises 9 trains, in this study, however, train 3 is not considered in this study due to unavailability of operating data, hence, 8 trains were considered.

Each train with a production capacity of approximately 7200 m^3d^{-1}. Trains 2, 5, 6, and 7 are installed with TM820L-440 membranes, while trains 1, 4, 8, and 9 are equipped with TM820S-400 membranes. Each train consists of a varying number of pressure vessels (PVs): trains 2, 5, 6, and 7 have 90 PVs, trains 1 and 4 have 80 PVs, and trains 8 and 9 have 79 PVs [30].

The membrane configuration in all trains includes 7 membranes per PV. The main purpose of this desalination plant is drinking water production. Table 2 provides detailed information on the membrane characteristics, including test conditions specified by the manufacturer, (pf = 5.52 MPa), $T_f = 25$ °C, $C_f = 32{,}000$ mg L^{-1}, flux recovery (R) = 8 % and pH = 8).

Both types of membranes feature a feed spacer thickness of $28{\cdot}10^{-3}$ in. To evaluate boron rejection, 5 mg L^{-1} of boron was intentionally added to the feedwater at a pH of 8. Table 3 shows feedwater inorganic composition indicating this feed boron concentration (C_{fB}) was above 5 mg L^{-1}. The conductivity of the feedwater ($Cond_f$) and permeate was measured using the EC 215 conductivity meter from Hanna® Instruments. The feedwater conductivity remained relatively stable, around 59,600 μS cm^{-1}, with a pH level averaging around 7. Temperature fluctuations in the feedwater for each train ranged between 18 and 26 °C for both types of membrane elements. A more detailed description of this desalination plant and data collection can be found in a previous work published by one of the authors [30].

The operating data collected and used for the dynamic ANN modeling as inputs were t, p_f, Q_f per PV, T_p, T_b, $Cond_f$, $Cond_p$, and R see Table 4.

The ANN-based model was proposed for predicting B_B. From the operating data, the mentioned permeability coefficients were calculated according to the solution-diffusion model. The calculation procedure for determining the permeability coefficients is described in detail in a previously published study [30]. It should be considered that the temperature correction factor (TCF) was not applied to calculate the experimental B_B as T_b and T_p were considered as inputs in the dynamic ANN-based model.

Additionally, in Table 5, an example of the data obtained in train number 1 can be seen. The rest of the trains work in the same way,

Table 2
Membrane characteristics according to the manufacturer [33].

Membrane	Product flow (m^3d^{-1})	NaCl rejection (%)	B rejection (%)
TM820S-400	34.1	99.75	90
TM820L-440	51.1	99.8	92

Table 3
Feed water inorganic composition.

Ion	Concentration (mg L^{-1})
Ca^{2+}	538
Mg^{2+}	1603
Na^{+}	12,675
K^{+}	468
HCO_3^-	164
SO_4^-	3740
NO_3^- < 0.005	<0.005
Cl^-	22,586
B	5.557
TDS	41,778

Table 4
Magnitudes, units, and types of data collected and used to form the SWRO plant data set.

Magnitude	Units	Type
t (1)	h	Input
p_f (2)	bar	Input
Q_f (3)	$m^3\,h^{-1}$	Input
Permeate temperature, (T_p) (4)	°C	Input
Brine temperature, (T_b) (5)	°C	Input
$Cond_f$ (6)	μS cm^{-1}	Input
$Cond_p$ (7)	μS cm^{-1}	Input
R (8)	%	Input

Table 5
Data collected in train 1 of 8 of the SWRO plant.

t	p_f	Q_f	T_p	T_b	$Cond_f$	$Cond_p$	Q_p
73	63,3	96,413	24,9	26,8	59,800	262	42,475
529	63,7	95,225	24,9	26,8	59,400	201	41,900
1369	67,5	96,750	20,2	21,3	59,300	184	42,625
1825	67,4	96,375	19,8	20,9	59,500	173	42,250
3337	71,8	88,638	19,5	20,6	59,200	243	39,383
3991	72,7	87,350	20,0	21,1	59,300	220	39,325
4303	71,1	90,613	20,6	21,7	59,300	223	40,600
4969	71,0	89,888	21,3	22,4	58,300	248	39,725
5472	70,9	90,325	23,1	24,2	58,900	259	40,625
6050	70,1	92,150	25,4	26,5	58,800	279	41,263
7225	67,2	97,250	24,5	25,6	55,900	289	43,950
7923	72,4	83,638	24,9	26,8	59,600	328	38,813
8522	72,5	87,125	20,8	22,9	59,200	313	39,313
9024	72,4	86,650	20,5	21,7	59,300	335	38,950
9697	68,5	96,413	20,1	19,7	57,900	303	43,225
10,223	69,5	93,463	19,4	18,9	58,400	309	41,813
10,680	68,2	95,675	19,7	18,8	58,400	307	43,025
11,207	71,0	89,875	19,8	18,7	57,900	362	40,625
12,217	70,4	91,063	20,4	19,9	57,800	378	41,163
13,056	69,5	92,538	20,9	20,2	57,300	440	41,850
14,951	68,4	95,388	23,3	24,9	57,600	608	43,000
16,151	68,4	94,625	23,2	24,3	57,500	680	42,500
17,087	68,2	94,500	21,9	23,6	58,900	664	42,750
20,255	72,0	87,250	19,9	20,5	56,900	722	39,380
20,815	73,0	86,875	20,2	20,8	56,700	776	39,250
21,600	72,8	85,875	20,3	21,1	55,700	763	38,750
22,107	74,1	84,750	21,0	21,7	57,400	976	38,250
23,279	72,8	87,375	24,0	25,0	58,300	1220	39,250
23,447	73,8	84,500	24,2	25,6	58,000	1190	38,250
23,879	67,6	97,750	24,8	25,0	58,000	948	41,000
25,203	70,5	91,625	23,1	24,9	59,000	1057	38,375
27,335	67,5	91,875	21,2	21,0	58,700	934	38,625
28,081	73,5	86,125	19,5	20,2	58,000	1056	36,750
28,777	71,5	89,375	19,5	20,2	57,600	1077	37,875

having a greater or lesser number of total data depending on the plant conditions.

2.2. Dynamic ANN model and network architecture

ANNs are computer systems inspired by the biological human brain. They work through a set of inputs used as training to learn patterns and predict or classify a series of new elements [34]. In this work, an ensemble of ANNs is used to forecast the rejection of boron as boric acid in a large-scale SWRO desalination plant. To get a full range of results, the model structure used is an ensemble of 1000 ANNs. These 1000 ANNs were selected after performing several experiments before this work to find the most stable forecast conditions. The closer to 1000 ANNs were ensembled, the more stable the results were. Also, each ANN contains a HL. This HL varies its number of neurons from 1 to N in each iteration (Fig. 1). N is defined as 5 since, as mentioned in the results section, from this value onwards, prediction success decreases.

2.3. Simulations

As explained above, the network is designed to perform an ensemble of 1000 individual ANNs. For the different trains of the SWRO desalination plant in the experiment the Holdout method was carried out. A range of 70–80 % of data (17–20 samples) are used to train the system (except for two lines that do have not enough data) and the rest is used to make the predictions and test the results.

At each iteration, each ANN changes its HL neurons from 1 to 5 and repeats the procedure 10 times to obtain a series of prediction values of B_B for each line. Selecting at the end the best output of the iterations.

From these values, the appropriate statistical parameters (Table 7) are obtained and the predicted value of B_B is compared with the actual value of B_B. Furthermore, the C_B values are calculated using the aforementioned Eq. (7). Then, these statistical parameters are compared with the values in the literature.

Several simulations have been carried out to obtain the best entry conditions in the ANN to predict B_B. These experiments are collected in Table 6. For this evaluation exist 10 types of conditions. The case with all the variables mentioned in Table 4 (t, p_f, Q_f per PV, T_p, T_b, $Cond_f$, $Cond_p$, and R) and the case with only 3 variables ($Cond_f$, $Cond_p$, and R). These 3 variables are selected because they present a high correlation with the real values of B_B according to the literature [30].

Therefore, considering the possibility of eliminating variables that contribute noise, variables that contribute more information to the classification according to the aforementioned bibliography are chosen as possible variables in experiments 6 to 10 in Table 6. In addition, three additional conditions are taken into account that is thought to provide added information; the boron value in the previous iteration (feedback), the time between experiments (time-lapse), and for the start of the experiment whether or not a first boron value input line was used (first line). The different cases that have been studied are shown in Table 6.

2.4. Statistical parameters

To assess the accuracy of the prediction of B_B as boric acid, a set of statistical parameters has been employed. The selection of these parameters is based on their widespread usage in the literature, which enables us to compare our findings with the current state of the art. The most prominent among them are *MSE*, *MAE*, and *MAPE*. Table 7 displays

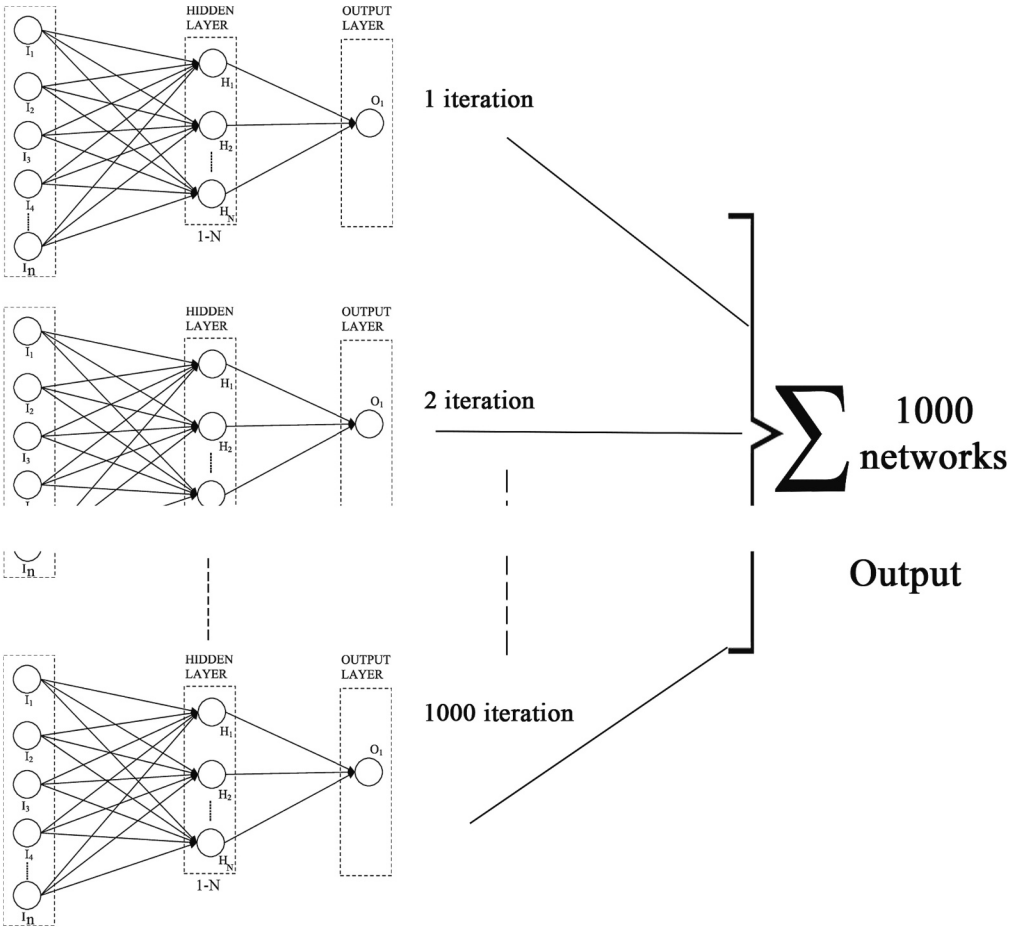

Fig. 1. Architecture of the ANN ensemble.

Table 6
Evaluation of the experiments to obtain the optimal entry conditions.[a]

Experiment conditions	Extra conditions		
	Feedback	Previous time lapse	First input line
All inputs (1) t, p_f, Q_f, T_p, T_b, $Cond_f$, $Cond_p$, R	No	No	No
All inputs (2) t, p_f, Q_f, T_p, T_b, $Cond_f$, $Cond_p$, R	Yes	Yes	Yes
All inputs (3) t, p_f, Q_f, T_p, T_b, $Cond_f$, $Cond_p$, R	No	Yes	Yes
All inputs (4) t, p_f, Q_f, T_p, T_b, $Cond_f$, $Cond_p$, R	Yes	No	Yes
All inputs (5) t, p_f, Q_f, T_p, T_b, $Cond_f$, $Cond_p$, R	Yes	Yes	No
Three inputs (6) $Cond_f$, $Cond_p$, R	No	No	No
Three inputs (7) $Cond_f$, $Cond_p$, R	Yes	Yes	Yes
Three inputs (8) $Cond_f$, $Cond_p$, R	No	Yes	Yes
Three inputs (9) $Cond_f$, $Cond_p$, R	Yes	No	Yes
Three inputs (10) $Cond_f$, $Cond_p$, R	Yes	Yes	No

[a] To simulate the best input conditions, only trains 1 and 5 were used (TM820S-400 membrane and TM820L-440 membrane, respectively). This is because we are looking for a representative case to find out the best input conditions and then carry out the simulations of the set of trains with those conditions, explained in Table 6.

Table 7
Parameters to evaluate B_B.

Parameter	Equation	
Average (Avg)	$\mathrm{X}\text{-} = \frac{\sum_{i=1}^{n} x_i}{N}$	(1)
Standard deviation (*STD*)	$\sigma = \sqrt{\frac{\sum_i^n (x_i - \mathrm{X})^2}{N}}$	(2)
MSE	$MSE = \frac{1}{n}\sum_{i=1}^{n}(y_i - \hat{y_i})^2$ y_i = *Observed values* $\hat{y_i}$ = *Predicted values*	(3)
RMSE	$RMSE = \sqrt{\frac{1}{n}\sum_{i=1}^{n}(y_i - \hat{y_i})^2}$	(4)
MAE	$MAE = \frac{1}{n}\sum_{i=1}^{n}\lvert y_i - \hat{y_i}\rvert$ y_i = *Observed values* $\hat{y_i}$ = *Predicted values*	(5)
MAPE	$MAPE = \frac{100}{n}\sum_{i=1}^{n}\frac{\lvert y_i - \hat{y_i}\rvert}{y_i}$ y_i = *Actual value* $\hat{y_i}$ = *Predicted value*	(6)

these parameters for reference:

2.5. Calculation of B_B

To calculate B_B, transport equation based on the solution diffusion model was used [35]. The flux of Boron (J_B) per unit area was determined using Eq. (7) as permeate flow (Q_P) and Boron concentration in the permeate (C_{pB}) were available from the experimental data. It should be mentioned that C_{pB} was estimated from $0.51 \cdot Cond_p$.

$$J_B = B_B\left(C_{mB} - C_{pB}\right) = \frac{Q_p C_{pB}}{S_m} \tag{7}$$

where C_{mB} is the Boron concentration (mg L^{-1}) on the membrane surface. To estimate this parameter, it is necessary to use Eq. (8) which is dependent on the polarization factor (*PF*). This parameter in turn depends on the permeate flux (J_p) and the mass transfer coefficient of Boron (k_B) (Eq. (9)). This mass transfer coefficient can be estimated from the solute mass transfer coefficient (k_s) from Eq. (11) [36]. This parameter was determined using Eqs. (12)–(20) [14].

$$C_{mB} = C_{fb-B} \cdot PF \tag{8}$$

$$PF = e^{J_p / k_B} \tag{9}$$

$$J_p = \frac{Q_p}{S_m} \tag{10}$$

$$k_B = k_s / 0.97 \tag{11}$$

$$k_s = \frac{D_{fb-s} Sh}{d_h} \tag{12}$$

$$D_{fb-s} = 6.725 \cdot 10^{-6} \cdot e^{\left(0.1546 \cdot 10^{-3} \cdot C_{fb-B} - \frac{2513}{273.15 + T_{fb}}\right)} \tag{13}$$

$$Sh = 0.14 \cdot Re^{0.64} \cdot Sc^{0.42} \tag{14}$$

$$Re = \frac{\rho_{fb} \cdot v_{fb} \cdot d_h}{\eta_{fb}} \tag{15}$$

$$\rho_{fb} = 498.4 \cdot m + \sqrt{248400 + 752.4 \cdot m \cdot C_{fb}} \tag{16}$$

$$m = 1.0069 - 2.757 \cdot 10^{-4} \cdot T_{fb} \tag{17}$$

$$\eta_{fb} = 1.234 \cdot 10^{-6} \cdot e^{\left(2.12 \cdot 10^{-3} \cdot C_{fb-B} - \frac{1965}{273.15 + T_{fb}}\right)} \tag{18}$$

$$d_h = \frac{4 \cdot \varepsilon}{\frac{2}{h} + (1 - \varepsilon)\frac{8}{h}} \tag{19}$$

$$Sc = \frac{\eta_{fb}}{\rho_{fb} D_{fb-s}} \tag{20}$$

$$B_B = \frac{Q_p C_{pB}}{TCF \cdot S_m \cdot \left(C_{fb-B} \cdot PF - C_{pB}\right)} \tag{21}$$

where B_B is the Boron permeability coefficient (m d^{-1}) at 25 °C, S_m is the membrane surface of each train, d_h (m) is the hydraulic diameter, $D_{fb\text{-}s}$ the feed-brine solute diffusivity (m^2 s^{-1}), Sh is the Sherwood number which correlation was taken from [14] taking into consideration the feed spacer geometry of the SWRO element used, *Sc* the Schmidt number, ρ_{fb} (kg m^{-3}) the feed-brine solution density, ν_{fb} the feed-brine velocity (m s^{-1}), η_{fb} (kg m^{-1} s^{-1}) the dynamic viscosity of the feed-brine solution, ε the porosity (0.89), h the feed spacer height.

3. Results and discussion

3.1. Relationship between input variables and outputs in ANN based model

To improve the accuracy of the model, we have performed a selection of the most significant input variables to analyze and eliminate those that do not provide relevant information, as discussed in Section 2.3 (simulations). According to the tests carried out in this work, $Cond_p$ has the strongest correlation with the real values of B_B ($R^2 = 0.9653$). This is because with the temporary degradation of the membrane, the $cond_p$ values will increase along with the B_B value. In order to confirm this, the temporal analysis of the variables is then performed. The rest of the variables show a correlation lower than 0.9, suggesting a non-linear correlation. These types of correlations are well captured by deep learning algorithms. It is also observed that the second highest

correlation is that of B_B with respect to time, which reinforces the idea that the rest of the variables have some kind of non-linear correlation. This is confirmed by the literature and the following tests [30]. Fig. 2 shows the different correlations between the value of B_B and the variables, together with their R^2 coefficient.

To further investigate the influence of the input variables on the prediction of B_B, we have analyzed the time evolution of their values. Our temporal analysis reveals that $Cond_p$, $Cond_f$, and R present a correlational evolution of their value over time, unlike the other variables (p_f, Q_f, T_p, T_b), which are apparently independent of time (Fig. 3). This suggests that as time passes, $Cond_p$ and R may be influenced by the membrane properties and, therefore, the values of B_B are influenced by them too, being correlated. This analysis of the time evolution of inputs in SWRO plants is complicated and presents difficulty in formulating hypotheses. Since there is no previous literature on data from an SWRO plant under operating conditions over several years.

Taking into account the relationship found in the equations of the literature cited in [30], and the results obtained from the temporal analysis and the relationship between inputs and output, we have selected three variables ($Cond_p$, $Cond_f$, and R) to study their influence on the prediction of B_B and, therefore, on the C_{pB}. These variables have been used as inputs in experiments 6–10 in Table 6, and we compare the B_B prediction with the cases where all variables are used as inputs (experiments 1–5 in Table 6). In Section 3.2, we present the results of this hypothesis and verify the validity of this approach. We conclude with a detailed analysis to determine the most suitable input variables to obtain accurate predictions of C_{pB} at the output of the ANN network.

3.2. Analysis of the best experiment conditions for inputs

A set of simulations has been conducted to predict the boron permeability coefficient (B_B) using various input conditions, as explained in Section 2.3 and shown in Table 6. Table 8 presents the best results for boron prediction, using all variables and experiment conditions 1 of Table 6. As described in Section 2.2, the experiment was repeated with varying HL neurons from 1 to N (where N = 5), resulting in a lower *MAE* and *MAPE* error at N = 2.

From this point, all simulations were performed using experiment condition 1, as other conditions yielded higher errors contrary to the hypothesis of Section 3.1 based on the linear correlations. The inputs to the ANN include all variables without feedback, time-lapse, or a sample of the previous boron line, as including these variables led to higher error rates, contrary to the findings in Section 3.1. Although the idea of using feedback and time lapses to collect data was initially considered, the collected data was found to have variable time intervals and limited significance. Moreover, the results with all variables as inputs showed that neural networks tend to benefit from more data, and all variables contain relevant information in the forecasting process, as opposed to the previous analysis in Section 3.1 to eliminate variables that do not provide information.

3.3. SWRO desalination plant simulation

The simulation was performed using the holdout method with the 8 lines (8 trains of the SWRO plant), with trains 1–4 using membrane TM820S-400 and trains 5–8 using membrane TM820L-440. Table 9 summarizes the results obtained for both types of membranes, including

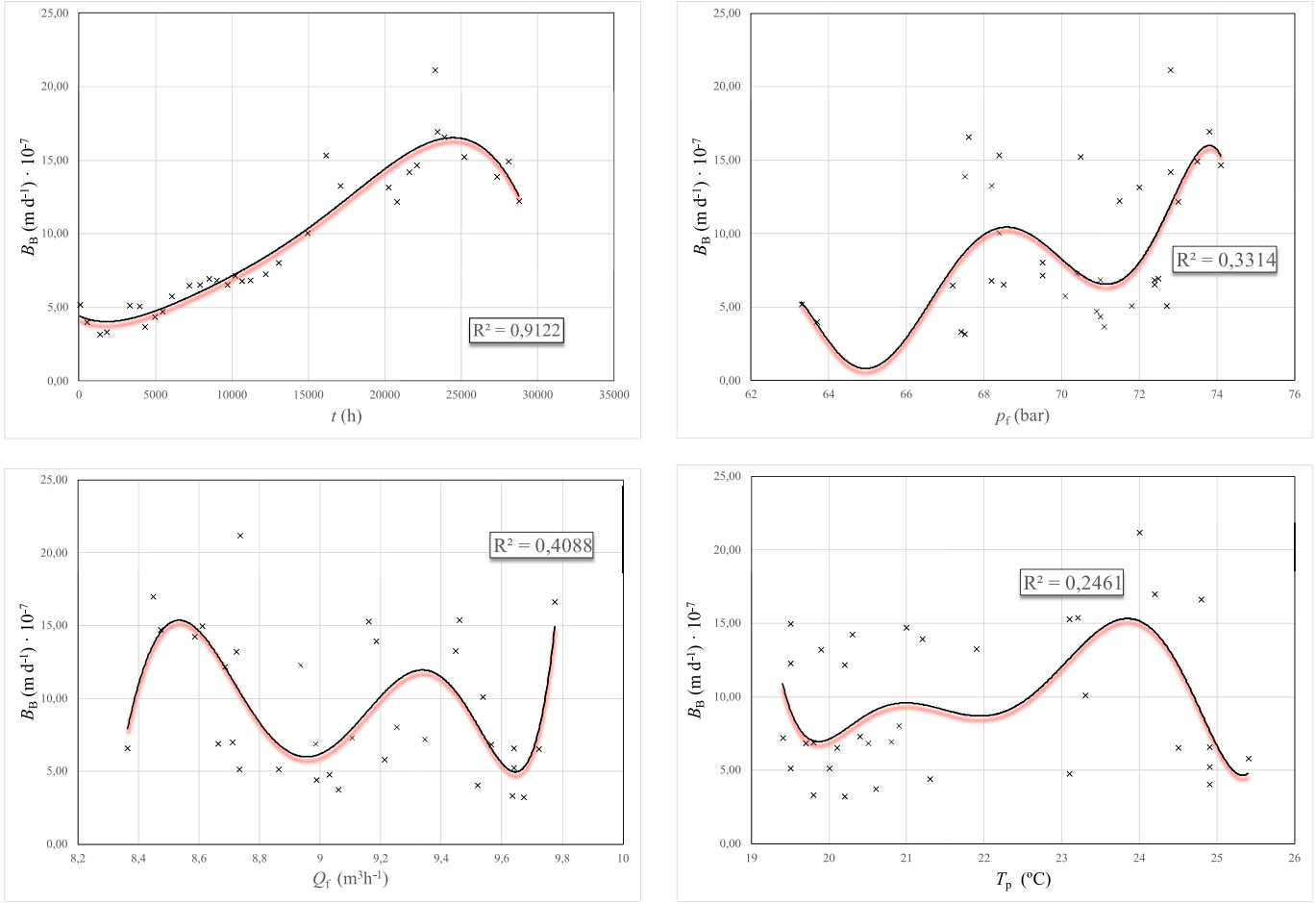

Fig. 2. Linear correlation between B_B and the variables.

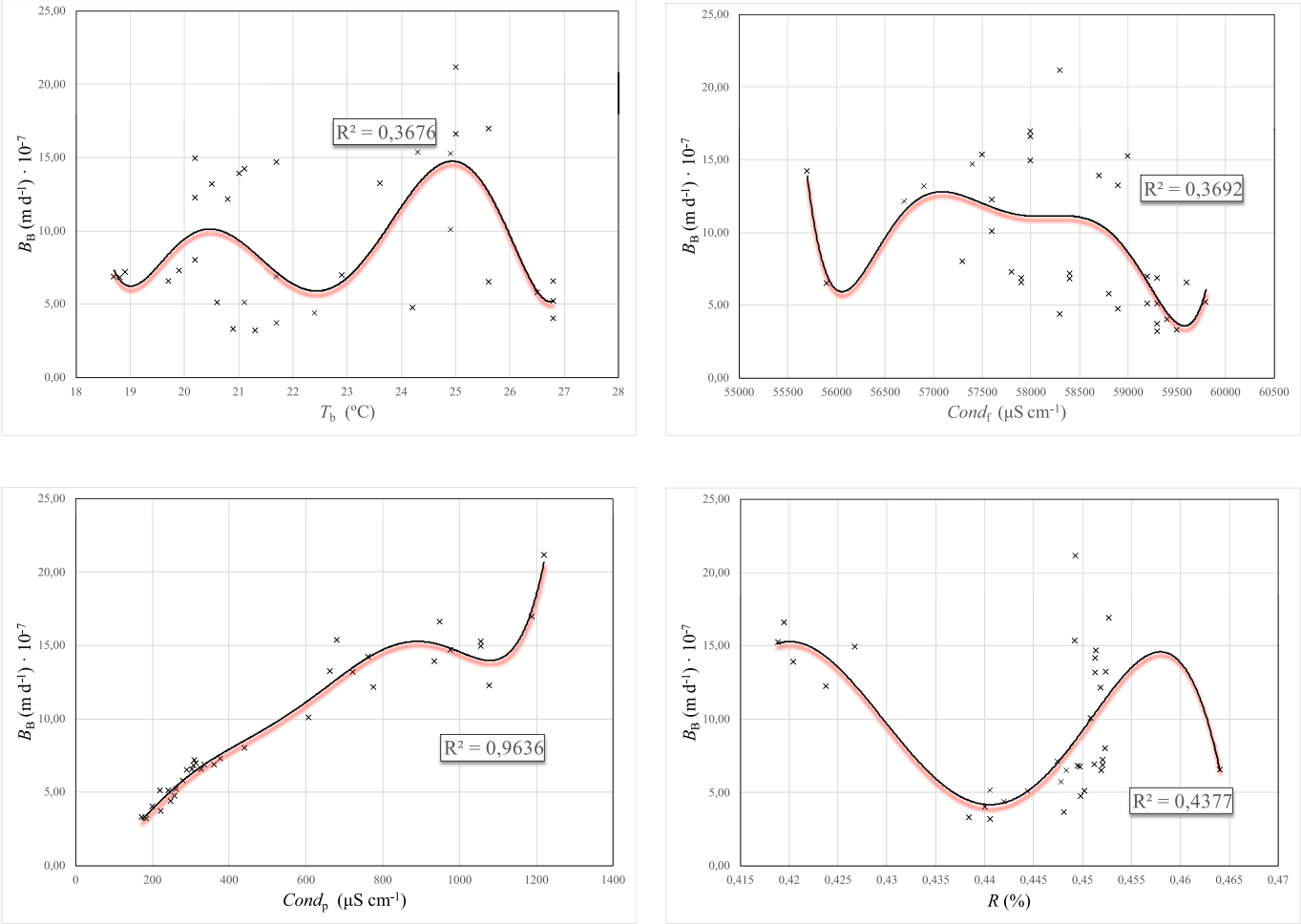

Fig. 2. (*continued*).

the averages for all 8 trains. The membrane used in trains 1–4 is more stable in predicting C_{pB}, with a *MAPE* of 11.2 % and a standard deviation of 1.65 %, while the membrane used in trains 5–8 has a higher *MAPE* (12.58 %) and standard deviation (4.59 %), resulting in worse prediction results for C_{pB}.

The best results were obtained for train 4 of membrane TM820S-400 and train 8 of membrane TM820L-440, with an average *MAPE* of 8.85 % and 6.06 % respectively, and an average difference between actual and estimated C_{pB} of 11.88 % and 6.05 % respectively. When analyzing the results, it is important to consider two factors: the differences between results on the same membrane and the differences between results of the two membranes. Differences in results of the same membrane can be attributed to two main reasons: the randomness of initial neuron weights and the amount of data used for training-test since more data generally leads to better predictions and not all trains have the same amount of data.

On the other hand, differences in results between the two membranes are due to variations in characteristics such as flow gdp, average NaCl rejection percentage, maximum pressure, and active area of the membrane. As a result, Boron rejection and RO are slightly different between the two membranes, leading to differences in prediction success.

Due to the limited availability of data from SWRO plants under operating conditions, the error values obtained through simulations of this nature are of limited comparability.

For instance, in previous works [19,20], the mean absolute percentage deviation of ion rejections predictions was between 3 % and 8 %, when operating under controlled laboratory conditions. However, in the present study, where full-scale operating conditions were used, a mean absolute standard deviation of 11.89 % was achieved, implying that despite the unfavorable conditions, the model responds adequately. Other works [21] reported a MAPE value below 2 % under laboratory conditions; however, standard deviation reached levels of up to 13 %, this compared with the system here proposed that reaches up values of 3.96 % on average in standard deviation, is a sign of the stability of the system.

Additionally, some works [29,33] reported excellent results, with a success rate in predicting ions in the output of over 99 %. However, these models were trained under laboratory conditions, with a dataset of fewer than 100 samples (where 80 % were used for training and only 10 % for the test). Therefore, although these results are very good, they cannot be compared to those presented in this study, where hundreds of data points were considered, all of them under large-scale operating conditions and from different trains.

In the light of the above, the B_B predictions made with the proposed model can be considered relatively favorable and allow to know the approximate value of the crucial parameters at the output, as well as to predict the C_{pB} level of boron concentration at the output. The short- and medium-term degradation of the membrane can also be analyzed indirectly. The feasibility of using the proposed model for short- and medium-term predictions is supported by the results presented in Fig. 4, which show a favorable agreement between the actual and predicted values of C_{BP}.

4. Conclusions

A novel approach to predicting boron rejection concentrations in

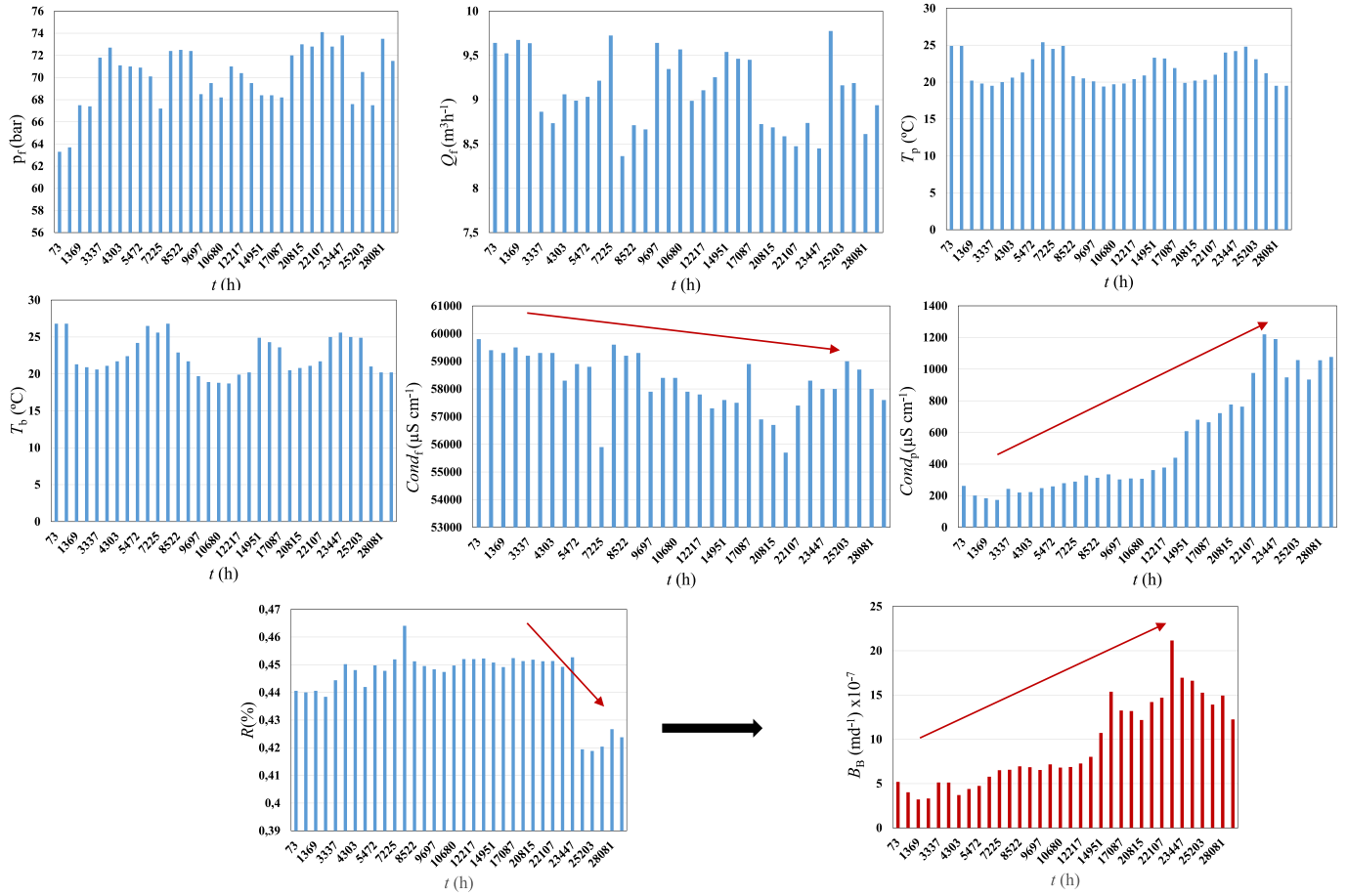

Fig. 3. Temporal evolution of the variables during >3 years in the SWRO plant.

Table 8
Statistical results of the best B_B prediction results are shown. The best case is using experiment conditions 1 in Table 6.

Experiment conditions 1 of Table 6 (all inputs)					
No. Iterations (10)	1 neuron in HL	2 neurons in HL	3 neurons in HL	4 neurons in HL	5 neurons in HL
STD	7.70×10^{-3}	1.03×10^{-2}	1.02×10^{-2}	1.04×10^{-2}	9.80×10^{-3}
MSE	8.86×10^{-14}	5.55×10^{-14}	5.13×10^{-14}	4.80×10^{-14}	4.82×10^{-14}
RMSE	2.16×10^{-7}	1.67×10^{-07}	1.72×10^{-07}	1.72×10^{-07}	1.75×10^{-07}
MAE	2.16×10^{-7}	1.66×10^{-07}	1.71×10^{-07}	1.71×10^{-07}	1.75×10^{-07}
MAPE	15.09	11.93	12.08	12.00	**12.22**

full-scale SWRO desalination plants using ensemble-based machine learning is presented in this study. While reverse osmosis is a leading technology in desalination, few studies have analyzed the performance of such plants under operating conditions. This work aims to fill this gap by developing and implementing machine learning algorithms for predicting boron permeability coefficient values in the permeate. The data analyzed comes from a reverse osmosis desalination plant in southeast Spain. The study seeks to analyze different types of variables and their weight in predicting these parameters. The results show that the system based on machine learning assembly can predict the boron permeability coefficient values with a certain margin of error, with MAE and MAPE values of $7.93{\cdot}10^{-8}$ and 11.8 % respectively, this error represents a deviation of approximately 0.1 mgL^{-1} in C_{pB} estimation. In contrast, a previous study utilized a data set obtained from an SWRO plant with 2 types of water-filtering membranes each one with 4 trains/lines. The data set was subsequently analyzed to obtain the most significant values, which were correlated and provided more information to a neural network architecture that had been developed. This ANN consisted of a dynamic ANN model that performed a set of 1000 individual ANNs. It then tried to predict future values of boron concentration at the membrane outlet. After the predictions, it was concluded that the inputs that gave the best result were p_f, Q_f, T_p, T_b, $Cond_f$, $Cond_p$ and R. A stable neural network architecture was designed whose inputs resulted in boron concentration predictions with a *MAPE* reaching values of 6 % and an average for the best membrane of 11.20 % ± 1.65 *MAPE*. A comparative study of the two membranes and the evolution of the prediction against time was carried out. The predictions of the B_B made with the proposed model are compared with other works carried out in the literature and are considered favorable, taking into account that all studies in the literature analyze laboratory conditions and have a reduced number of samples, unlike the one proposed here.

This study provides a model capable of predicting the B_B value in the permeate, using operational variables. This makes it possible to predict the level of boron concentration in the permeate and therefore to know its evolution in the short and medium term, which facilitates the understanding of the process and can help in carrying out operations or substitutions in the plant. This work is novel due to the inclusion of artificial intelligence algorithms in the field of water purification under operating conditions in SWRO desalination plants. It serves as a stepping stone for future research in applying automatic and deep learning methods in water purification.

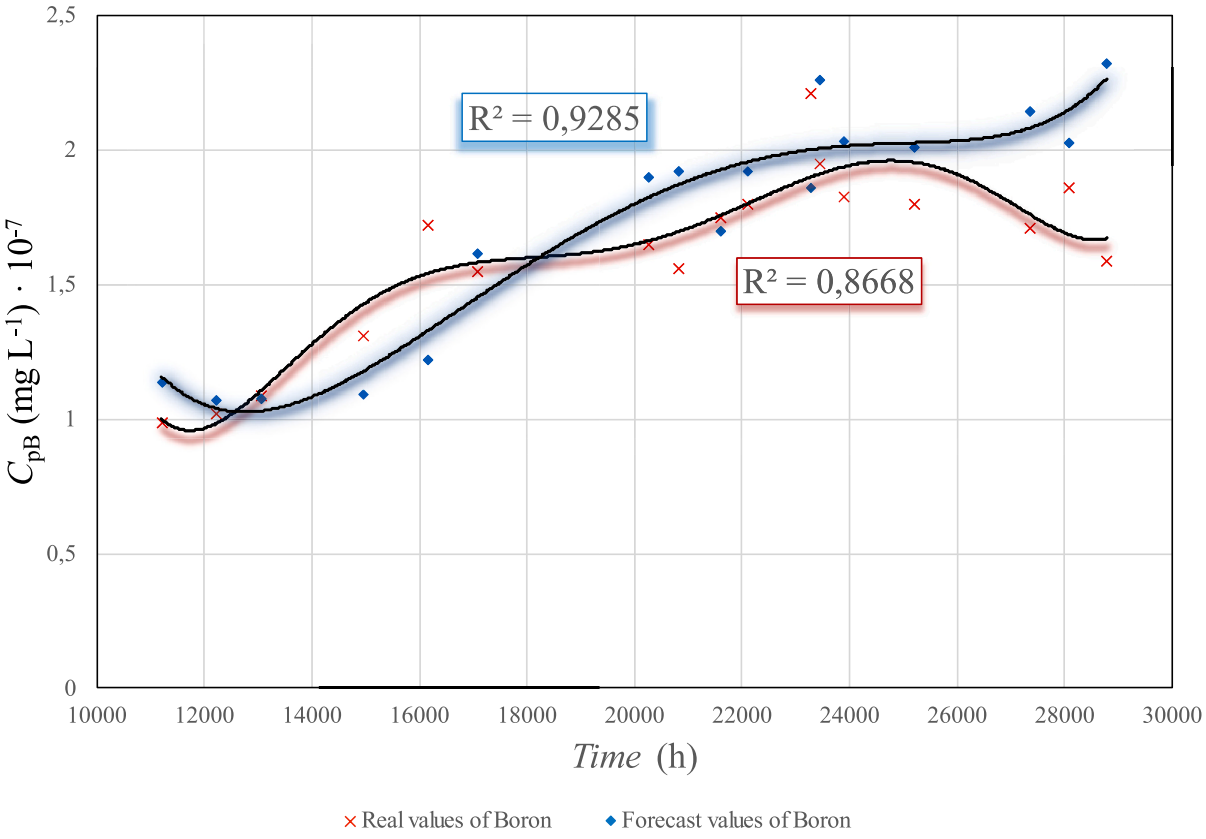

Fig. 4. Actual and predicted C_B values.

Declaration of competing interest

The authors declare that they have no known competing financial interests or personal relationships that could have appeared to influence the work reported in this paper.

Data availability

Data will be made available on request.

References

[1] M. Qasim, M. Badrelzaman, N.N. Darwish, N.A. Darwish, N. Hilal, Reverse osmosis desalination: a state-of-the-art review, Desalination 459 (2019) 59–104, https://doi.org/10.1016/J.DESAL.2019.02.008.
[2] A. Zapata-Sierra, M. Cascajares, A. Alcayde, F. Manzano-Agugliaro, Worldwide research trends on desalination, Desalination 519 (2021), 115305, https://doi.org/10.1016/J.DESAL.2021.115305.
[3] A. Ruiz-García, I. Nuez, Long-term performance decline in a brackish water reverse osmosis desalination plant. Predictive model for the water permeability coefficient, Desalination 397 (2016) 101–107, https://doi.org/10.1016/J.DESAL.2016.06.027.
[4] F.E. Ahmed, A. Khalil, N. Hilal, Emerging desalination technologies: current status, challenges, and future trends, Desalination 517 (2021), 115183, https://doi.org/10.1016/J.DESAL.2021.115183.
[5] A.M. Aish, H.A. Zaqoot, S.M. Abdeljawad, Artificial neural network approach for predicting reverse osmosis desalination plants performance in the Gaza Strip, Desalination 367 (2015) 240–247, https://doi.org/10.1016/J.DESAL.2015.04.008.
[6] A. Ruiz-García, I. de la Nuez-Pestana, A computational tool for designing BWRO systems with spiral wound modules, Desalination 426 (2018) 69–77, https://doi.org/10.1016/J.DESAL.2017.10.040.
[7] N. Najid, J.N. Hakizimana, S. Kouzbour, B. Gourich, A. Ruiz-García, C. Vial, Y. Stiriba, R. Semiat, Fouling control and modeling in reverse osmosis for seawater desalination: a review, Comput. Chem. Eng. 162 (2022), 107794, https://doi.org/10.1016/J.COMPCHEMENG.2022.107794.
[8] L.A. Richards, M. Vuachère, A.I. Schäfer, Impact of pH on the removal of fluoride, nitrate and boron by nanofiltration/reverse osmosis, Desalination 261 (2010) 331–337, https://doi.org/10.1016/J.DESAL.2010.06.025.
[9] N. Najid, S. Kouzbour, A. Ruiz-Garcia, S. Fellaou, B. Gourich, Y. Stiriba, Comparison analysis of different technologies for the removal of boron from seawater: a review, J. Environ. Chem. Eng. 9 (2021), 105133, https://doi.org/10.1016/J.JECE.2021.105133.
[10] Y.J. Lim, K. Goh, M. Kurihara, R. Wang, Seawater desalination by reverse osmosis: current development and future challenges in membrane fabrication – a review, J. Membr. Sci. 629 (2021), 119292, https://doi.org/10.1016/J.MEMSCI.2021.119292.
[11] C. Wang, M.J. Park, H. Yu, H. Matsuyama, E. Drioli, H.K. Shon, Recent advances of nanocomposite membranes using layer-by-layer assembly, J. Membr. Sci. 661 (2022), 120926, https://doi.org/10.1016/J.MEMSCI.2022.120926.
[12] N. Jeong, T. Chung, T. Tong, Predicting micropollutant removal by reverse osmosis and nanofiltration membranes: is machine learning viable? Environ. Sci. Technol. 55 (2021) 11348–11359, https://doi.org/10.1021/acs.est.1c04041.
[13] M.T. Mito, X. Ma, H. Albuflasa, P.A. Davies, Variable operation of a renewable energy-driven reverse osmosis system using model predictive control and variable recovery: towards large-scale implementation, Desalination 532 (2022), 115715, https://doi.org/10.1016/J.DESAL.2022.115715.
[14] A. Ruiz-García, I. Nuez, M.D. Carrascosa-Chisvert, J.J. Santana, Simulations of BWRO systems under different feedwater characteristics. Analysis of operation windows and optimal operating points, Desalination 491 (2020), 114582, https://doi.org/10.1016/J.DESAL.2020.114582.
[15] Z. Zhou, D.A. Ladner, Computational modeling of discrete-object feed spacers attached directly onto reverse osmosis membranes for enhanced module packing capacity and improved hydrodynamics, Sep. Purif. Technol. 300 (2022), 121727, https://doi.org/10.1016/J.SEPPUR.2022.121727.
[16] S. Al Aani, T. Bonny, S.W. Hasan, N. Hilal, Can machine language and artificial intelligence revolutionize process automation for water treatment and desalination? Desalination 458 (2019) 84–96, https://doi.org/10.1016/J.DESAL.2019.02.005.
[17] J. Jawad, A.H. Hawari, S. Javaid Zaidi, Artificial neural network modeling of wastewater treatment and desalination using membrane processes: a review, Chem. Eng. J. 419 (2021), 129540, https://doi.org/10.1016/J.CEJ.2021.129540.
[18] W.R. Bowen, M.G. Jones, J.S. Welfoot, H.N.S. Yousef, Predicting salt rejections at nanofiltration membranes using artificial neural networks, Desalination 129 (2000) 147–162, https://doi.org/10.1016/S0011-9164(00)00057-6.
[19] N.A. Darwish, N. Hilal, H. Al-Zoubi, A.W. Mohammad, Neural networks simulation of the filtration of sodium chloride and magnesium chloride solutions using

nanofiltration membranes, Chem. Eng. Res. Des. 85 (2007) 417–430, https://doi.org/10.1205/CHERD06037.
[20] H. Al-Zoubi, N. Hilal, N.A. Darwish, A.W. Mohammad, Rejection and modelling of sulphate and potassium salts by nanofiltration membranes: neural network and Spiegler–Kedem model, Desalination 206 (2007) 42–60, https://doi.org/10.1016/J.DESAL.2006.02.060.
[21] V. Yangali-Quintanilla, A. Verliefde, T.U. Kim, A. Sadmani, M. Kennedy, G. Amy, Artificial neural network models based on QSAR for predicting rejection of neutral organic compounds by polyamide nanofiltration and reverse osmosis membranes, J. Membr. Sci. 342 (2009) 251–262, https://doi.org/10.1016/J.MEMSCI.2009.06.048.
[22] L. Khaouane, Y. Ammi, S. Hanini, Modeling the retention of organic compounds by nanofiltration and reverse osmosis membranes using bootstrap aggregated neural networks, Arab. J. Sci. Eng. 42 (2017) 1443–1453, https://doi.org/10.1007/s13369-016-2320-2.
[23] Z.V.P. Murthy, M.M. Vora, Prediction of reverse osmosis performance using artificial neural network, (2004).
[24] D. Libotean, J. Giralt, F. Giralt, R. Rallo, T. Wolfe, Y. Cohen, Neural network approach for modeling the performance of reverse osmosis membrane desalting, J. Membr. Sci. 326 (2009) 408–419, https://doi.org/10.1016/J.MEMSCI.2008.10.028.
[25] M. Khayet, C. Cojocaru, M. Essalhi, Artificial neural network modeling and response surface methodology of desalination by reverse osmosis, J. Membr. Sci. 368 (2011) 202–214, https://doi.org/10.1016/J.MEMSCI.2010.11.030.
[26] S.S. Madaeni, M. Shiri, A.R. Kurdian, Modeling, optimization, and control of reverse osmosis water treatment in Kazeroon power plant using neural network, Chem. Eng. Commun. 202 (2015) 6–14, https://doi.org/10.1080/00986445.2013.828606.
[27] Y. Choi, Y. Lee, K. Shin, Y. Park, S. Lee, Analysis of long-term performance of full-scale reverse osmosis desalination plant using artificial neural network and tree model, Environ. Eng. Res. 25 (2020) 763–770.
[28] A. Adda, S. Hanini, S. Bezari, M. Laidi, M. Abbas, Modeling and optimization of small-scale NF/RO seawater desalination using the artificial neural network (ANN), Environ. Eng. Res. 27 (2022).
[29] R. Mahadeva, M. Kumar, S.P. Patole, G. Manik, Employing artificial neural network for accurate modeling, simulation and performance analysis of an RO-based desalination process, Sustain. Comput.: Inform. Syst. 35 (2022), 100735, https://doi.org/10.1016/J.SUSCOM.2022.100735.
[30] A. Ruiz-García, F.A. León, A. Ramos-Martín, Different boron rejection behavior in two RO membranes installed in the same full-scale SWRO desalination plant, Desalination 449 (2019) 131–138, https://doi.org/10.1016/J.DESAL.2018.07.012.
[31] Y. LeCun, Y. Bengio, G. Hinton, Deep learning, Nature 521 (2015) 436–444, https://doi.org/10.1038/nature14539.
[32] W. Zaremba, I. Sutskever, O. Vinyals, Recurrent Neural Network Regularization, ArXiv Prepr. ArXiv1409.2329, 2014.
[33] H. Salem, A.E. Kabeel, E.M.S. El-Said, O.M. Elzeki, Predictive modelling for solar power-driven hybrid desalination system using artificial neural network regression with Adam optimization, Desalination 522 (2022), 115411, https://doi.org/10.1016/J.DESAL.2021.115411.
[34] Z.R. Yang, Z. Yang, Artificial neural networks, Compr. Biomed. Phys. 6 (2014) 1–17, https://doi.org/10.1016/B978-0-444-53632-7.01101-1.
[35] J.G. Wijmans, R.W. Baker, The solution-diffusion model: a review, J. Membr. Sci. 107 (1995) 1–21, https://doi.org/10.1016/0376-7388(95)00102-I.
[36] M. Taniguchi, M. Kurihara, S. Kimura, Boron reduction performance of reverse osmosis seawater desalination process, J. Membr. Sci. 183 (2001) 259–267, https://doi.org/10.1016/S0376-7388(00)00596-2.